Glucose-Induced Oxidative Stress in Vascular Contractile Cells

Comparison of Aortic Smooth Muscle Cells and Retinal Pericytes

Peter C. Sharpe, Wei-Hua Liu, Kevin K.M. Yue, Dorothy McMaster, Mark A. Catherwood, Ann M. McGinty, and Elisabeth R. Trimble

Free radical–mediated damage to vascular cells may be involved in the pathogenesis of diabetic vasculopathy. The aim of this study was to compare the extent of glucose-induced oxidative stress in both vascular smooth muscle cells (VSMCs) and pericytes and the effect on antioxidant enzyme gene expression and activities. Porcine aortic VSMC and retinal pericytes were cultured in either 5 or 25 mmol/l glucose for 10 days. Intracellular malondialdehyde (MDA) was measured as a marker of peroxidative damage, and mRNA expression of CuZn-SOD, MnSOD, catalase, and glutathione peroxidase (GPX) were measured by Northern analysis. Glutathione (GSH) was also measured. There was a significant increase in MDA in VSMCs in 25 mmol/l glucose (1.34 ± 0.11 vs. 1.88 ± 0.24 nmol/mg protein, 5 vs. 25 mmol/l D-glucose, mean $\pm$ SE, $n = 15$, $P < 0.01$), but not in pericytes (0.38 ± 0.05 vs. 0.37 ± 0.05 nmol/mg protein, $n = 11$). There was a significant decrease in GSH in both cell types (VSMC, 1.40 ± 0.13 vs. 0.69 ± 0.12 nmol/mg protein, $n = 15$, $P < 0.001$; pericytes, 1.97 ± 0.17 vs. 0.94 ± 0.16 nmol/mg protein, $n = 11$, $P < 0.001$). mRNA expression of CuZnSOD and MnSOD was increased only in VSMCs (by 58.5 ± 8.1 and $41.0 \pm 6.9\%$, respectively, $n = 8$, $P < 0.01$). CuZnSOD protein was increased by ~120% ($P < 0.00001$). None of the antioxidant enzyme activities was altered between 5 and 25 mmol/l glucose in either cell type. Both MnSOD activities and GSH concentrations were higher in pericytes compared with VSMC under basal (5 mmol/l) conditions ($P < 0.05$ and $P < 0.02$, respectively). These results demonstrate glucose-induced reduction of GSH in both cells, but only in VSMC is there evidence of oxidant damage in the form of lipid peroxidation, implying significant differences in intracellular responses to glucose between contractile cells in the macro- and microvasculature. *Diabetes* 47:801–809, 1998

Long-term vascular complications represent the main cause of morbidity and mortality in diabetic patients and occur in both the micro- and macrovasculature. Cardiovascular disease is the leading cause of mortality in patients with diabetes (1), and myocardial infarction and stroke account for 80% of all deaths in patients with type 2 diabetes (2). Proliferative retinopathy, a major cause of blindness, is present in 25% of patients with type 1 diabetes after 15 years and in more than 50% after 20 years (3). Diabetic nephropathy develops in about 35% of patients with type 1 diabetes and leads to chronic renal failure (4).

The pathogenesis of diabetic vasculopathy is highly complex, and there may be differences between disease affecting the macrovasculature and that affecting the microvasculature. However, the major primary metabolic abnormality that causes both is hyperglycemia. The outcome of the Diabetes Control and Complications Trial (5) resolved the issue of whether chronic hyperglycemia is an important factor in microvasculopathy, and other studies also demonstrated its importance in macrovascular disease (6). Vascular pathology involves both functional and structural changes in the endothelial layer, such as altered endothelium-dependent dilatation (7) and reduced endothelial cell proliferation (8). Alterations may occur in the extracellular matrix; in particular, increased concentrations of fibronectin, laminin, and collagen IV have been described (9,10). Increased VSMC growth and proliferation in the arterial intima is one key feature of atherosclerosis (11), and increased proliferation has also been demonstrated in VSMC cultured in high concentrations of glucose (8,12). In contrast to VSMC hyperproliferation, loss of pericytes has been reported in diabetes, associated with the development of retinal microvascular lesions (13).

Although the pathogenesis of diabetic vasculopathy is probably multifactorial in origin, studies suggest a role for glucose-induced oxidative stress (14). There are many ways by which hyperglycemia may increase the generation of free

radicals, such as glucose autoxidation (15), autoxidative glycosylation (glycoxidation) (16), activation of protein kinase C (17), and increased polyol pathway metabolism with subsequent "pseudohypoxia" (18). There is also evidence that elevations in glucose concentrations may depress natural antioxidant defenses such as vitamin C (ascorbate) (19) and glutathione (20). In keeping with evidence of oxidative stress, it has been reported that indirect markers of free radical damage—such as malondialdehyde (MDA), a marker of lipid peroxidation—are elevated in patients with diabetes (19,21,22).

It is well-established that prokaryotic organisms and eukaryotic cells have the ability to modulate gene expression as a function of oxygen tension and exposure to reactive oxygen species. Several different endogenous antioxidant enzymes—superoxide dismutase (SOD), catalase, and glutathione peroxidase (GPX)—protect cells against the damaging effects of reactive oxygen species. SOD catalyzes the dismutation of superoxide to hydrogen peroxide and exists in three main subforms: cytosolic copper/zinc SOD (CuZn-SOD), mitochondrial manganese SOD (MnSOD), and extracellular SOD (EC-SOD). Catalase is a ubiquitous enzyme present in peroxisomes; it catalyzes the two-stage conversion of hydrogen peroxide to water and oxygen. GPX is a selenoprotein found in both the cytoplasm and the mitochondria (23); it reduces lipidic or nonlipidic hydroperoxides as well as hydrogen peroxide while oxidizing two molecules of glutathione (GSH; 24). Therefore, GPX requires GSH to detoxify peroxides, and when GSH is oxidized to glutathione disulfide (GSSG), it is subsequently reduced back to GSH by the enzyme glutathione reductase (GR). It is generally believed that the exposure of cells and organisms to increased oxidative stress is associated with an increase in antioxidant enzyme activity, particularly that of the SOD enzymes (25,26). With regard to gene (mRNA) expression of antioxidant enzymes under conditions of oxidative stress, increases in MnSOD mRNA expression have been reported (27). However, increases in CuZnSOD mRNA expression have also been reported in both endothelial cells and VSMCs exposed to hyperoxia (28). Therefore, increased gene expression and activities of antioxidant enzymes can be taken as evidence of exposure to increased oxidative stress.

In diabetes, where glucose-induced oxidative stress is believed to play an important role in tissue damage and complications, relatively little research has been conducted on the defenses of vascular cell antioxidant enzymes. Studies have demonstrated impairment of endothelium-dependent relaxations in diabetic animals and humans (endothelial dysfunction) (7), which can be reversed by antioxidants (29). High glucose concentrations have also been noted to reduce endothelial cell numbers, and again these alterations can be reversed by antioxidants (30). Exposure of human endothelial cells to 20 mmol/l D-glucose for 7 and 14 days was associated with an increase in the mRNA expression of CuZnSOD, MnSOD, catalase, and GPX and a corresponding increase in the enzyme activities (31). All of the above findings suggest that diabetes or glucose-induced endothelial dysfunction may be related to free radical–mediated damage.

The role of glucose-induced oxidative stress and its potentially damaging effects on the contractile cells of both the macrovasculature (VSMCs) and the microvasculature (pericytes in the retinal circulation) have not previously been evaluated. The aim of this study was to identify the existence of glucose-induced oxidative stress in both VSMCs and pericytes and to investigate its subsequent effects on antioxidant enzyme gene expression and activities. GSH is a key endogenous aqueous phase antioxidant, and we therefore assessed the effects of high glucose concentrations and/or oxidative stress on its intracellular concentration.

RESEARCH DESIGN AND METHODS

Cell culture

VSMCs. All reagents were obtained from Sigma Chemical (Poole, Dorset, U.K.) unless otherwise stated. Porcine aorta was obtained from the local abattoir. By blunt dissection, the intima and adventitial layers of a segment of the descending aorta were stripped and discarded. The medial segment was then cut into small pieces of ~1 mm^2 and transferred onto the growing surface of 25 cm^2 tissue culture flasks (Corning; Bibby Sterilin, Staff, U.K.) that were premoistened with fetal calf serum (FCS; PAA Laboratories, Linz, Austria). Each flask contained 15–20 pieces. Then Dulbecco's modified Eagle's medium (DMEM; GibcoBRL, Life Technologies, Paisley, U.K.) containing 25 mmol/l HEPES, 1 mmol/l sodium pyruvate, 5 mmol/l D-glucose, and 2 mmol/l glutamine and supplemented with antibiotics (benzylpenicillin 60 μg/ml, streptomycin sulfate 100 μg/ml), amphotericin B (2.5 μg/ml, GibcoBRL) and 10% (vol/vol) FCS (growth medium) was added to the flasks. The flasks were placed in an incubator with their growing surface uppermost at 37°C with a 5% CO$_2$/95% air atmosphere for 24 h to ensure explant adhesion. After inversion of the flasks, the growth medium (DMEM/10% FCS) was replaced twice weekly. VSMCs grew out from the explants within 7–10 days, reaching confluence within 2–3 weeks, and were harvested with 0.125% trypsin (type II, porcine pancreas; Difco Laboratories, Detroit, MI) containing 0.01% Na$_2$-EDTA (BDH Chemicals, Poole, Dorset, U.K.) in phosphate-buffered saline (PBS; pH 7.4) and split for further culture into 75 cm^2 tissue culture flasks (Corning). Cells were confirmed as VSMC by their typical morphology and positive immunofluorescence staining with a monoclonal antibody against smooth muscle α-actin.

For the different experiments, cells were cultured for 10 days in the growth medium plus either 5 mmol/l (normal) or 25 mmol/l (high) D-glucose. When results of analyses (described below) demonstrated significant differences between 5 mmol/l and 25 mmol/l D-glucose, VSMCs were also cultured in the presence of 5 mmol/l D-glucose + 20 mmol/l L-glucose (extracellular glycation control) and 5 mmol/l D-glucose + 20 mmol/l mannitol (osmotic control). Growth medium was changed twice weekly. All experiments were performed on cells up to and including subculture number 5. VSMCs were serum-starved for 12–16 h before each experiment.

Retinal pericytes. Primary culture and subculture of porcine retinal pericytes were established as previously described (32). Briefly, porcine eyes were obtained from the local abattoir and the retinas isolated and homogenized in DMEM. The homogenate was filtered through a 85-μm nylon mesh. The trapped microvessels were digested in an enzyme cocktail (pronase, deoxyribonuclease, and collagenase) in PBS for 5 min, filtered through a 53-μm nylon mesh, and plated in 25 cm^2 tissue culture flasks (Corning) in DMEM containing 20% FCS. Pericytes formed a confluent monolayer within 14 days and were identified by morphological criteria and by positive staining with smooth muscle α-actin using immunocytochemical techniques. The lack of staining to monoclonal anti–factor VIII and polyclonal anti-endothelin in such cultures was used to confirm the absence of endothelial cells.

Subculturing of pericytes was as described for VSMC above. Subcultures one to four were used in all experiments. The cells were maintained in identical conditions to those of VSMC for a period of 10 days.

Viability of cultures. Trypan blue solution (0.4%, Sigma) was added to aliquots of cell suspensions in a 1:1 ratio. The suspension was mixed and allowed to stand for 10 min at room temperature. A hemocytometer was used to count live and dead cells, and viability percentages were calculated. Lactate dehydrogenase activities were also measured in the supernatants using dry-film technology on a Vitros 750 analyzer (Johnson and Johnson Clinical Diagnostics, Amersham, Bucks, U.K.).

Harvesting of VSMCs and pericytes for antioxidant enzyme activities and measurement of MDA and GSH. The monolayers were rinsed twice with ice-cold Hanks' balanced salt solution (without calcium and magnesium and phenol red; GibcoBRL), and the cells were collected using a disposable cell scraper (Sarstedt, Leicester, U.K.). The cells were centrifuged at 225g at 4°C for 5 min, and the cell pellet was stored at 80°C before the stage of cell lysis and release of cell and organelle contents.

Cell lysis and homogenization. Cell pellets were removed from the –80°C freezer, maintained at room temperature for 4–5 min, and resuspended in 0.1% Triton X-100 (BDH Chemicals) in PBS (pH 7.4). Sonication was performed with two 15-s bursts on a Lucas Dawe sonicator (Lucas Dawe Ultrasonics, London, U.K.),

using a microtip (setting number 4, continuous cycle) with a 20-s cooling period separating the two bursts. At this stage, an aliquot of the cell homogenate was removed for protein analysis. The rest of the homogenate was centrifuged at 3,000*g* for 30 min at 4°C, and aliquots of the resulting supernatant were taken for SOD (CuZnSOD and MnSOD), catalase, and GPX activities, CuZnSOD protein concentration, and MDA and GSH concentrations. Analyses of enzymatic activities were performed immediately. MDA samples were stored at –80°C prior to analysis. The samples for GSH concentration required further treatment to maintain stability; this involved the addition of one part 10% sulphosalicylic acid (Sigma) to two parts sample. The sample was mixed and centrifuged at 13,000*g* for 5 min. The supernatant was removed and stored at –80°C before analysis.

Protein measurement. Total protein analysis was performed using a bicinchoninic acid protein assay reagent kit (Pierce and Warriner, Chester, U.K.). All results of antioxidant enzyme activities, MDA, and GSH were standardized against cell protein concentration.

MDA. MDA was measured by high-performance liquid chromatography with fluorimetric detection by the method of Young and Trimble (33).

Antioxidant enzyme activities

GPX. The enzyme activity of GPX was determined in the cell extracts by the method of McMaster et al. (34).

Superoxide dismutase. Total SOD activity was measured using a modification of the method of L'Abbe and Fischer (35) adapted for the Cobas Fara centrifugal analyzer (Roche, Welwyn Garden City, Herts, U.K.). This method primarily measures CuZnSOD activity because at pH 10 the apparent activity of CuZnSOD in the assay increases approximately 10-fold compared with that observed at pH 7.8, whereas the apparent MnSOD activity is the same at both pH levels (35,36). Total SOD activity was measured initially, followed by MnSOD activity, which is resistant to incubation with 2 mmol/l potassium cyanide (BDH Chemicals) at room temperature for 45 min. CuZnSOD activity was subsequently calculated by the subtraction of MnSOD activity from total SOD activity.

Catalase. The peroxidatic function of catalase was measured by the method of Johansson and Borg (37) adapted for automation on the Cobas Fara centrifugal analyzer (38).

CuZnSOD protein concentration. CuZnSOD protein concentration was measured using an enzyme-linked immunosorbent assay (ELISA). The primary antibody, polyclonal rabbit anti-superoxide dismutase (bovine erythrocyte) antibody, was purchased from Chemicon (Temecula, CA); the secondary antibody, horse radish peroxidase conjugated goat anti-rabbit polyclonal antibody, was obtained from Dako (High Wycombe, Bucks, U.K.). All other materials were obtained from Sigma unless otherwise stated.

Initial assessment of antibody reactivity. Antigen was immobilized on uncoated microtitration strips (Wallac U.K., Milton Keynes, U.K.). CuZnSOD from bovine erythrocytes was used for the standards and was diluted in 10 mmol/l borate buffer (pH 9.6). Two hundred microliters of standard was added to a well in the microtitration strip and immobilized by incubation at room temperature for 16 h. Cell homogenates were diluted in borate buffer and similarly incubated overnight. After the immobilization step, the wells were washed twice with wash solution (Wallac U.K.) on an automated microtiter plate washer, and 200 µl of PBS (pH 7.4) containing 1% bovine serum albumin (BSA) was added and incubated for 30 min at room temperature to block free binding sites. The wells were subsequently washed twice (wash solution), and 200 µl of primary antibody (1:1,000) diluted in PBS/1% BSA was added to each well and incubated, with shaking, for 2 h at room temperature. Then the wells were again washed twice (wash solution), and 200 µl of the secondary antibody diluted in PBS/1% BSA was added (1:5,000); incubation was for 2 h, with shaking, at room temperature, after which the wells were again washed twice (wash solution). Next, 200 µl of substrate solution was added, which was prepared as follows: phosphate-citrate buffer was prepared by the addition of an appropriate volume of 58 mmol/l Na$_2$HPO$_4$ solution to 100 ml of 13.7 mmol/l citric acid solution to give a final pH of 5.6. To 15 ml of phosphate-citrate buffer was added 3.75 mg *o*-phenylenediamine (free base) and 7.1 µl of 30% hydrogen peroxide (substrate solution). The microtitration strips were incubated at room temperature for 20 min in the dark. At the end of this period, 50 µl of stop reagent (2 mol/l H$_2$SO$_4$) was added to each well and the absorbance read on a Novo Biolabs microtiter plate reader (Novo Nordisk, Cambridge, U.K.) at 490 nm. Initial results indicated the presence of measurable CuZnSOD protein in the samples. All standards and samples were run in duplicate on each occasion.

Optimization of ELISA for CuZnSOD. To establish the standard curve, initial experiments using 1:10 repeated dilutions of CuZnSOD standards from 10 mg/l to 0.1 ng/l demonstrated that the maximum slope of the standard curve occurred from approximately 1 to 100 µg/l. However, further work established the relatively linear portion to be from ~1 to 30 µg/l.

Sensitivity was calculated from three times the standard deviation of the zero standard (blank). Using 20 repeated zero standard absorbance readings, the sensitivity was calculated at 0.41 µg/l.

The standards were purified bovine erythrocyte CuZnSOD and the samples were porcine in origin; therefore, it was impossible to assess the cross-reactivity of the

primary antibody with the porcine samples. However, there is a high degree of homology between porcine and bovine CuZnSOD (~90%). In measuring CuZnSOD protein, the main interest was in comparing the results between subgroups (5 vs. 25 mmol/l D-glucose), rather than absolute concentrations. The secondary antibody itself demonstrated no cross-reactivity with standard or samples in the absence of primary antibody incubation.

The following coefficients of variation (CVs) were obtained with each sample assayed in five replications on five different occasions: intra-assay CV was 2.5–4.1%, inter-assay CV was 13.2–15.0% (2, 4, and 8 µg/l).

For recovery, cell samples were spiked with known concentrations of bovine erythrocyte CuZnSOD. The mean recovery of CuZnSOD (bovine erythrocyte) was 94.4 ± 4.6% (2 µg/l) and 92.8 ± 5.8% (5 µg/l; n = 5).

Matrix effects were assessed by serial dilutions of five cell homogenate samples. This demonstrated linearity in dilution and indicated that there was no significant matrix interference in the assay.

Glutathione. This was measured by the method described by Griffith (39), which was modified and automated on the Cobas Fara centrifugal analyzer. The assay detects both GSH and GSSG. GSSG was assayed separately using 2-vinylpyridine (2-VP), which reacts with and effectively masks GSH but not GSSG in the analysis. On account of GSSG's low concentration, each measurement of GSSG required combining of cells from six 75 cm^2 flasks.

RNA extraction. Total cellular RNA was extracted from cultured cells using the acid-guanidinium thiocyanate-phenol-chloroform method of Chomczynski and Sacchi (40).

Northern blot analysis. Aliquots (30 µg) of total RNA from cells cultured in 5 and 25 mmol/l D-glucose were separated by electrophoresis on a 1% agarose-formaldehyde gel. Transfer of the denatured RNA was accomplished by capillary elution to a charged nylon filter (Hybond N+; Amersham, Little Chalford, Bucks, U.K.).

Hybridization was carried out in a Tecne Hybridizer HB-1D hybridization oven (Techne, Duxford, Cambridge, U.K.) using specific porcine cDNA probes to CuZnSOD, MnSOD, and GPX mRNA and a human cDNA probe to catalase mRNA prepared by reverse-transcriptase–polymerase chain reaction (RT-PCR) as described in the following section. A porcine cDNA probe to glyceraldehyde-3 phosphate dehydrogenase (GAPDH) was also prepared by RT-PCR and used as a "housekeeping" gene. The membrane was placed into a hybridization cylinder and pre-hybridized at 65°C for 30 min following the addition of Quickhyb hybridization solution (0.2 ml/cm^2; Stratagene, Cambridge, U.K.). cDNA probes (75–100 ng) were labeled using the Prime-It II Random Primer Labelling kit (Stratagene) and 50 µCi ^{32}P dCTP (Amersham; Redivue, 370 MBq/ml). Hybridization was carried out for a period of 2 h at 65°C (60°C for catalase). After this, the membrane was washed (at 42°C) twice for 15 min in 2× sodium chloride–sodium citrate (SSC), 0.1% SDS; once for 15 min with 1× SSC, 0.1% SDS; and finally for 15 min with 0.2× SSC, 0.1% SDS.

The washed membranes were subsequently analyzed on a Bio-Rad Molecular Imager (phosphorimager) system GS-525 (Bio-Rad, Hemel Hempstead, Herts, U.K.). Band intensities were quantified, using the attached software, by volume analysis with local background subtraction.

RT-PCR. cDNA probes for porcine CuZnSOD, MnSOD, GPX, GAPDH, and human catalase were prepared by RT-PCR, using primers designed to amplify a specific sequence. Protein and nucleotide sequences were obtained from GenBank (Los Alamos, NM). The following PCR primers were used (*Eco*RI internal restriction sites are underlined):

1. *MnSOD* (Acc. No. X64057);
   CBS1: GGAATTCCAGCTGCACCACAGCGAGC (100 pmol/reaction)
   CBA1: GGAATTCGATCCCCAGCAGCGGAACC (100 pmol/reaction)
2. *CuZnSOD* (Acc. No. P04178)
   CBS2: GGAATTCT(T/C)CA(T/C)GTNCA(T/C)CA(A/G)TT(T/C)GG
   (640 pmol/reaction)
   CBA2: GGAATTCC(A/G)TCNGG(T/C)TT(T/C)TC(A/G)TGNAC
   (1,280 pmol/reaction)
3. Catalase (Acc. No. P04040)
   CBS18: GGAATTCTTCGACCCAAGCAACATGC (100 pmol/reaction)
   CBA18: GGAATTCCTTGTCCAGAAGAGCCTGG (100 pmol/reaction)
4. GPX I (41-43)
   CBS3: GGGAATTCCCNTG(T/C)AA(T/C)CA(A/G)TT(T/C)GG
   (320 pmol/reaction)
   CBA3: GGGAATTCG(T/C)(T/C)T(C/G)(A/G/T)AT(A/G)TCNGG(T/C)TC
   (1,290 pmol/reaction)
5. GAPDH (Acc. Nos. U48832, X94251)
   CBS4: GGGAATTCACNATGGA(A/G)AA(A/G)GCNGG (320 pmol/reaction)
   CBA4: GGAATTCTTGGAGGCCATGTGGACC (100 pmol/reaction)

Oligo(dT) primed first-strand cDNA synthesis was carried out on total RNA (1 µg, porcine RNA for CuZnSOD, MnSOD, GPX, and GAPDH, human skin fibroblast RNA for catalase) using a reverse transcription system (Promega, Madison, WI)

but with superscript II Rnase H⁻ reverse transcriptase (GibcoBRL). PCR reagents were obtained from Promega unless otherwise stated. An aliquot (3 µl) of the first-strand cDNA reaction was added directly to the PCR mix containing 0.25 mmol/l of each deoxynucleotide triphosphate (dATP, dCTP, dGTP, dTTP), 5.0 U Taq DNA polymerase, and sense and antisense primers in 100 µl of 1× Taq DNA polymerase buffer (50 mmol/l KCl, 10 mmol/l Tris-HCl [pH 9.0], 0.1% Triton X-100). MgCl$_2$ was added to a final concentration of 1.5 mmol/l. A Perkin Elmer DNA Thermal Cycler (Perkin Elmer, Beaconsfield, Bucks, U.K.) was used with the following cycling times and temperatures: 94°C for 2 min; 5 cycles of 50°C for 1 min, 72°C for 40 s, and 94°C for 45 s; 30 cycles of 60°C for 1 min, 72°C for 40 s, and 94°C for 45 s; and then 72°C for 5 min. Reaction products (10 µl) were separated by 1.0–2.0% agarose gel electrophoresis in 1× TAE buffer and visualized by staining with ethidium bromide (0.5 µg/ml).

From the design of primers and the known nucleotide and protein sequences, it was possible to predict the molecular size of the expected PCR product. These were as follows: MnSOD, 405 bp; CuZnSOD, 243 bp; GPX, 354 bp; catalase, 512 bp; GAPDH, 690 bp.

Purification of PCR products was performed using the Wizard PCR purification kit (Promega) and subcloned into pGEM-T (Promega). Verification of transformation was performed by PCR screening of individual colonies (clones). The sequence of cDNA inserts was verified. Plasmid DNA was denatured and sequenced in both directions using sequenase V2.0 (USB, Cleveland, OH).

Statistical analysis. Comparison between 5 and 25 mmol/l glucose was performed using either paired t tests or the nonparametric Wilcoxon's signed-rank test. The normality of data was determined by the Kolmogorov-Smirnov normality test. The paired t test was used to compare the results of Northern analyses. Differences between VSMCs and pericytes (5 mmol/l glucose) were compared using unpaired t tests or Mann-Whitney U tests. Results are expressed as means ± SE unless otherwise stated.

RESULTS

Cell viability. There were no significant differences in cell viability between cells cultured in either 5 or 25 mmol/l D-glucose as assessed by trypan blue exclusion (at least 91% of cells were viable in all conditions). There were also no increases in lactate dehydrogenase activity in the supernatants under any condition (results not shown).

Evidence of lipid peroxidation as assessed by MDA. Intracellular MDA concentrations were significantly higher (by 40%) in VSMCs cultured in 25 mmol/l D-glucose compared with those cultured in 5 mmol/l D-glucose (1.34 ± 0.11 vs. 1.88 ± 0.24 nmol/mg protein, 5 vs. 25 mmol/l D-glucose, n = 15, P < 0.01) (Fig. 1). This increase was not seen in VSMCs cultured in the presence of 5 mmol/l D-glucose + 20 mmol/l L-glucose (glycation control) or 5 mmol/l D-glucose + 20 mmol/l mannitol (osmotic control) (1.18 ± 0.13 and 1.28 ± 0.15 nmol/mg protein, respectively, n = 15). However, in pericytes, 25 mmol/l D-glucose did not cause an increase in MDA (0.38 ± 0.05 vs. 0.37 ± 0.05 nmol/mg protein, 5 vs. 25 mmol/l D-glucose, n = 11), and pericytes had significantly lower values of MDA (P < 0.01) than did VSMCs at both glucose concentrations.

GSH. Because GSSG represents less than 3% of total glutathione in both VSMCs and pericytes cultured in 5 and 25 mmol/l glucose (reported below), total glutathione can be used as a measure of GSH (Fig. 2). When cultured in 5 mmol/l D-glucose, GSH levels of pericytes were 40% higher than those of VSMCs (P < 0.02). In 25 mmol/l D-glucose, GSH was reduced by 50% in both VSMCs (1.40 ± 0.13 vs. 0.69 ± 0.12 nmol/mg protein, 5 vs. 25 mmol/l D-glucose, n = 15, P < 0.001) and pericytes (1.97 ± 0.17 vs. 0.94 ± 0.16, n = 11, P < 0.001). The decrease in GSH demonstrated in the presence of 25 mmol/l D-glucose was not found in VSMCs or pericytes grown either in 5 mmol/l D-glucose + 20 mmol/l L-glucose or in 5 mmol/l D-glucose + 20 mmol/l mannitol (results not shown).

In a further set of experiments where each measurement required the combining of cells from six 75 cm² tissue culture
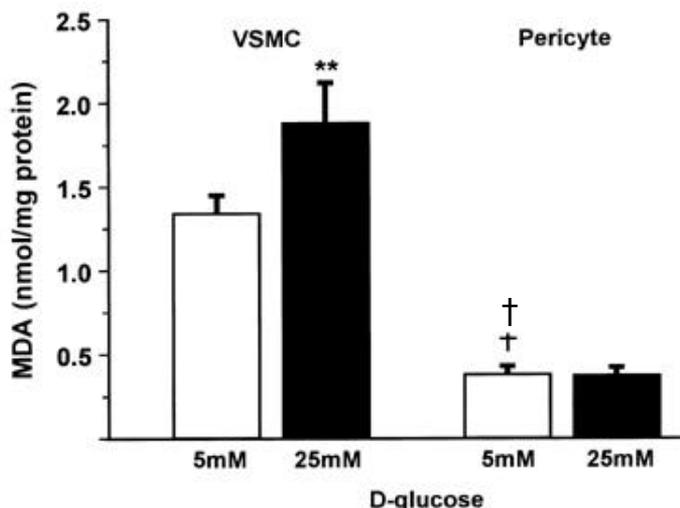

FIG. 1. Intracellular MDA in VSMCs and pericytes cultured in 5 and 25 mmol/l D-glucose for 10 days. **P < 0.01 compared with 5 mmol/l D-glucose; †P < 0.01, 5 mmol/l (pericyte) vs. 5 mmol/l (VMSC). n = 15 independent experiments for VSMCs; n = 11 independent experiments for pericytes.

flasks (Table 1), GSSG concentrations were <3% of the total GSH in both VSMCs and pericytes (n = 3 for both) cultured in 5 and 25 mmol/l D-glucose. There was no increase of GSSG in 25 mmol/l D-glucose.

mRNA expression of endogenous antioxidant enzymes. Figure 3 shows the PCR products for the antioxidant enzymes obtained after RT-PCR. The results of mRNA expression for each of the antioxidant enzymes are displayed in Table 2, and a typical example is shown in Fig. 4. When the volume of the mRNA expression of 5 mmol/l D-glucose is taken as 100%, the results demonstrate significant increases in the mRNA expression of both CuZnSOD and MnSOD in VSMCs cultured in 25 mmol/l D-glucose (by 58.5 and 41.0%, respectively); no differences were found in VSMC catalase or
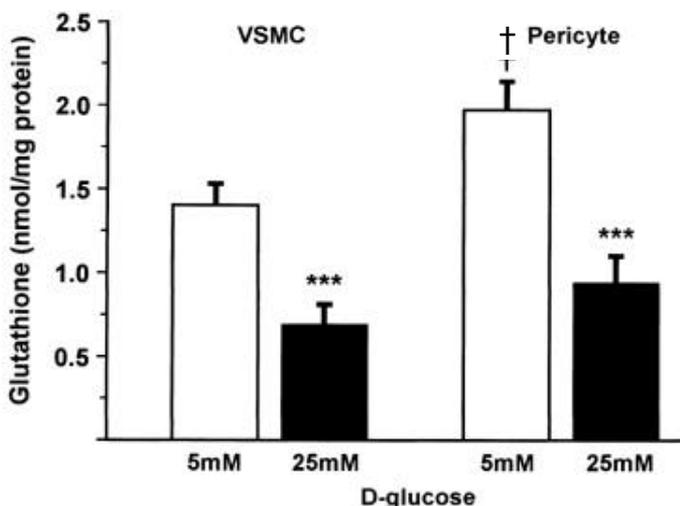

FIG. 2. Intracellular GSH in VSMCs and pericytes cultured in 5 and 25 mmol/l D-glucose for 10 days. ***P < 0.001 compared with 5 mmol/l D-glucose; †P < 0.02, 5 mmol/l (pericyte) vs. 5 mmol/l (VSMC). n = 15 independent experiments for VSMCs; n = 11 independent experiments for pericytes.

TABLE 1
GSSG in VSMCs and pericytes cultured for 10 days in 5 and 25 mmol/l D-glucose

	GSSG (nmol/mg protein)		GSH (nmol/mg protein)	
	5 mmol/l glucose	25 mmol/l glucose	5 mmol/l glucose	25 mmol/l glucose
VSMC	0.042 ± 0.006	0.025 ± 0.004	1.98 ± 0.17	0.89 ± 0.12
Pericyte	0.041 ± 0.004	0.030 ± 0.008	2.39 ± 0.38	1.05 ± 0.25

Data are means $\pm$ SE. $n = 3$ independent experiments for both VSMC and pericyte. GSSG was <3% of total glutathione under all conditions.

GPX, nor in any of the enzyme mRNAs in the pericyte. The increase in mRNA expression of CuZnSOD and MnSOD in VSMCs cultured in 25 mmol/l D-glucose did not occur in the presence of either 5 mmol/l D-glucose + 20 mmol/l L-glucose or 5 mmol/l D-glucose + 20 mmol/l mannitol (Table 3).

Antioxidant enzyme activities. Results of antioxidant enzyme activities are demonstrated in Table 4 and show no significant differences in activities between 5 and 25 mmol/l D-glucose for either VSMCs or pericytes. However, when pericytes were compared with VSMCs (5 mmol/l D-glucose), MnSOD activities were significantly higher ($P < 0.05$) and GPX activities were significantly lower ($P < 0.05$).

CuZnSOD protein concentration. This was measured in VSMCs only in view of the increase in mRNA expression of CuZnSOD in these cells when cultured in 25 vs. 5 mmol/l D-glucose. The ELISA has been validated by us (see METHODS), and Fig. 5 shows a typical standard curve. CuZnSOD protein concentration was significantly increased in 25 mmol/l D-glucose (3.88 ± 0.29 vs. 8.53 ± 0.44 ng/mg protein, $n = 15$, $P < 0.00001$; Fig. 6). CuZnSOD protein was not increased in the presence of 5 mmol/l D-glucose + 20 mmol/l L-glucose or of 5 mmol/l D-glucose + 20 mmol/l mannitol (results not shown).

DISCUSSION

The increased intracellular MDA found in VSMCs cultured in the presence of high concentrations of glucose is indicative of intracellular lipid peroxidation and oxidant-induced damage. The fact that the MDA level did not increase in peri-

cytes under the influence of increased glucose concentrations may be due, at least in part, to the higher levels of both GSH in the cytosol and MnSOD in the mitochondria of pericytes under control conditions. The lower basal levels of MDA in pericytes compared with VSMCs may also be explained by the same mechanism; however, differences in membrane fatty acid composition between cells could be a more important factor. MDA arises from the oxidative degradation of polyunsaturated fatty acids with more than two methylene-interrupted double bonds, particularly arachidonic acid (20:4) and docosahexaenoic acid (22:6) (44). Hyperglycemia may increase the generation of free radicals in many ways, such as glucose autoxidation, autoxidative glycosylation (glycoxidation), increased polyol pathway metabolism with subsequent "pseudohypoxia," and decreases in natural antioxidant defenses.

GSH is one of the most important intracellular antioxidants, associated with a recycling mechanism that converts the oxidized form, GSSG, back to GSH; the recycling mechanism provides a multiplier effect on the total antioxidant capacity of the system. GSH levels were significantly higher in pericytes than in VSMCs under basal conditions. In the presence of high glucose, there was an approximate 50% reduction of GSH in both cell types without any increase in the proportion of GSSG present. The reason for the reduction in GSH in both VSMCs and pericytes remains unclear. Thiol groups possess antioxidant properties (45), and GSH is a major source of thiol groups in the intracellular com-
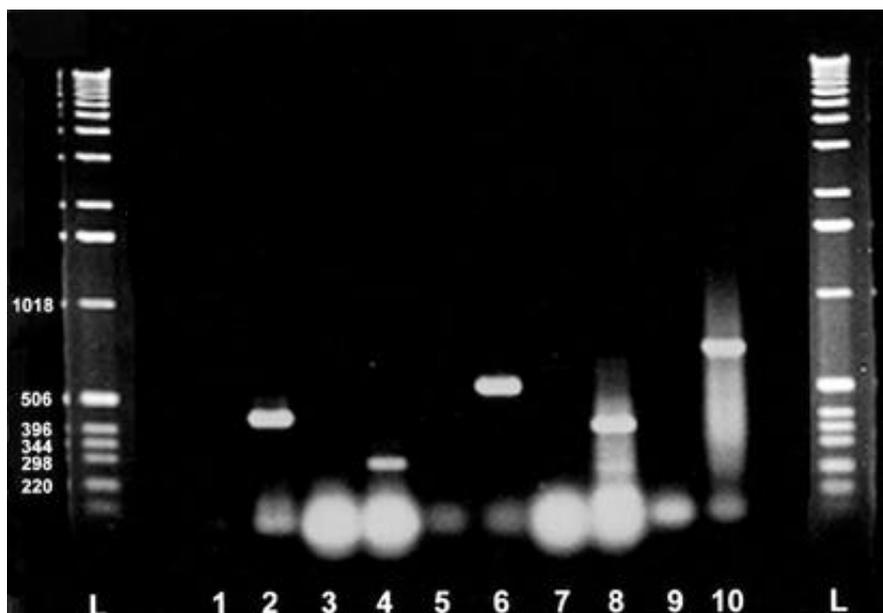

FIG. 3. RT-PCR products. After RT-PCR, reaction products were separated on a 1.5% agarose gel and visualized by staining with ethidium bromide (0.5 µg/ml). L = 1 kb DNA ladder (with key size markers indicated, bp). *Lanes 1* and *2*, MnSOD (–/+ cDNA); *lanes 3* and *4*, CuZnSOD (–/+ cDNA); *lanes 5* and *6*, catalase (–/+ cDNA); *lanes 7* and *8*, GPX (–/+ cDNA); *lanes 9* and *10*, GAPDH (–/+ cDNA). Molecular sizes were as predicted in METHODS: MnSOD, 405 bp; CuZnSOD, 243 bp; catalase, 512 bp; GPX, 354 bp; and GAPDH, 690 bp.

TABLE 2
VSMCs and pericytes: mRNA expression of antioxidant enzymes in VSMCs and pericytes after culture for 10 days in 25 mmol/l D-glucose compared with 5 mmol/l D-glucose (100%)

Antioxidant enzyme mRNA expression	VSMC (25 mmol/l D-glucose)	Pericyte (25 mmol/l D-glucose)
CuZnSOD	158.5 ± 8.1%* (8)	99.6 ± 4.4% (5)
MnSOD	141.0 ± 6.9%* (8)	98.6 ± 7.8% (5)
Catalase	102.3%, 107.0% (2)	104.6%, 120.7% (2)
GPX	113.3 ± 4.9% (8)	101.6 ± 4.5% (5)
GAPDH	105.7 ± 4.9% (8)	104.3 ± 5.8% (5)

Data are means ± SE (number of independent experiments) except for catalase, where two individual results are given. *$P < 0.01$ compared with 5 mmol/l D-glucose.
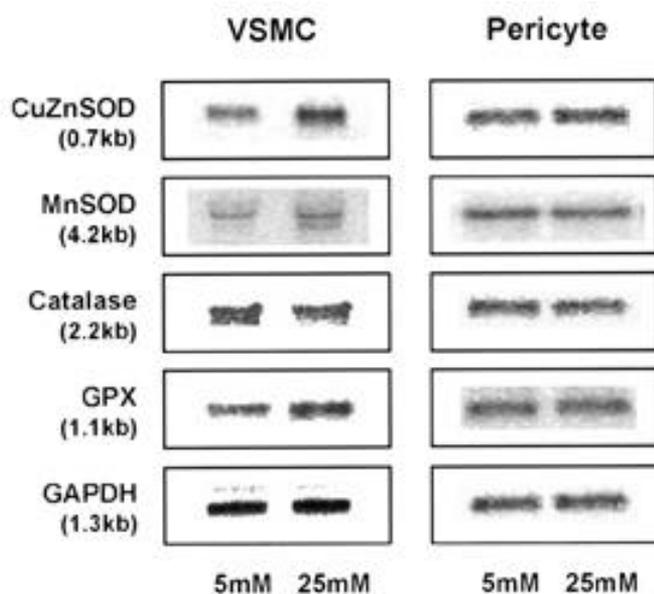

FIG. 4. mRNA expression of antioxidant enzymes (CuZnSOD, MnSOD, catalase, and GPX) and GADPH in VSMCs and pericytes cultured in 5 and 25 mmol/l D-glucose in a representative experiment.

partment. GSH reacts with aldehydes produced during peroxidation of lipids, protecting the thiol groups of membrane proteins (46). Under conditions of oxidative stress, GSH is oxidized to GSSG, and this reaction is catalyzed by GPX. GSSG is subsequently converted back to GSH by GR through the coupling reaction of NADPH to NADP (47). Under normal circumstances, >99.5% of total glutathione is GSH and <0.5% is GSSG, but there is a tendency for the GSSG:GSH ratio to increase in oxidative stress. The situation is complicated by the fact that export of GSH and possibly GSSG (48) from the cell may be increased in conditions of oxidative stress, leading to difficulties in the interpretation of the GSSG:GSH ratio. Export of GSH from the cell is a normal physiological process that accounts for cellular utilization of GSH (49) and appears to function as part of a system for the protection of cell membranes. Active transport of GSSG has been reported in several cell types, including erythrocytes (50), hepatocytes, and cardiac muscle cells (51). It has not been determined whether this transport system exists in VSMCs or pericytes. The GSSG:GSH ratio is therefore governed by the rate of synthesis of GSH, the prevailing oxidative state, the activities of GPX and GR, and the degree of export of GSH and GSSG from the cell. It has been consistently reported that GSH is decreased in patients with diabetes (52,53). Various mechanisms may be responsible for this decrease, including reduced activity of GR secondary to polyol pathway activation and, hence, reduced NADPH availability; reduced activity of the key rate-limiting enzyme in GSH synthesis, γ-glutamylcysteine synthetase (γ-GCS) may also be involved (54). Yoshida et al. (20) reported a decrease in activity of γ-GCS in erythrocytes from 15 type 2 diabetic subjects and in both mRNA expression and activity

of γ-GCS in human erythroleukemic cells cultured in high glucose concentrations. These effects were prevented by aminoguanidine, suggesting that glucose-derived modification of γ-GCS could be one of the mechanisms in predisposing the cells to oxidative injury. Trocino et al. (55) also reported a decrease in GSH in rat embryos exposed to conditions of high ambient glucose and associated oxidative stress. The reduction in GSH found in our experiments, therefore, could be either a primary (reduced synthesis) or a secondary (increased usage/export) event.

A significant increase in mRNA for CuZnSOD and MnSOD was found only in VSMC where a reduction of GSH was found at the same time as evidence of lipid peroxidation. It seems reasonable to suggest that increased gene expression for these enzymes is an adaptive response of the cell in an attempt to increase antioxidant defense capacity. The increase in mRNA was associated with a greater than twofold increase in CuZnSOD protein concentration in VSMC. The experiments have not addressed the exact mechanism by which glucose alters antioxidant defenses. The postulated mechanisms (see above) could lead to increased free radical production in the cytosolic compartment and to increased superoxide ion formation secondary to leakage of electrons from the electron transport chain in mitochondria

TABLE 3
VSMC only: mRNA expression of CuZnSOD and MnSOD cultured for 10 days in the presence of 25 mmol/l D-glucose, 5 mmol/l D-glucose + 20 mmol/l L-glucose, or 5 mmol/l D-glucose + 20 mmol/l mannitol compared with 5 mmol/l D-glucose (100%)

Antioxidant enzyme mRNA expression	25 mmol/l D-glucose	5 mmol/l D-glucose + 20 mmol/l L-glucose	5 mmol/l D-glucose + 20 mmol/l mannitol
CuZnSOD	154.5 ± 8.5%	109 ± 10.0%	114 ± 8.5%
MnSOD	146 ± 8.0%	93 ± 11.0%	111 ± 6.5%
GAPDH	109.5 ± 4.0%	107.5 ± 6.5%	96.5 ± 7.0%

Data are means ± SE. n = 3 independent experiments.

TABLE 4
Intracellular antioxidant enzyme activities in VSMC and pericytes cultured for 10 days in 5 and 25 mmol/l D-glucose

Antioxidant enzyme activities	VSMC		Pericyte	
	5 mmol/l glucose	25 mmol/l glucose	5 mmol/l glucose	25 mmol/l glucose
CuZnSOD (U/mg protein)	65.9 ± 3.7	65.1 ± 3.9	33.5 ± 3.6	35.8 ± 3.2
MnSOD (U/mg protein)	3.1 ± 0.4	3.0 ± 0.3	16.2 ± 3.2*	13.0± 0.9
Catalase (U/mg protein)	12.1 (6.7–31.9)	12.9 (5.8–32.3)	8.4 ± 0.l5	9.9 ± 0.3
GPX (mU/mg protein)	14.6 ± 2.2	17.3 ± 2.9	1.5 ± 0.8*	0.7 ± 0.3

Data are means ± SE, except for catalase, which are median (range) in the case of VSMC. *$P < 0.05$, 5 mmol/l (pericyte) vs. 5 mmol/l (VSMC). $n = 15$ for VSMC; $n = 5$ for pericytes. Please note that both CuZnSOD and MnSOD activities in the standard assay are measured at pH 10; this increases the activity of CuZnSOD by ~10-fold and has no effect on the activity of MnSOD when compared with measurements made at pH 7.8. The activities of MnSOD (mitochondrion) and catalase (peroxisome) have been normalized against total cell protein.

(56). With the above changes in mRNA and protein concentration for CuZnSOD in VSMCs, it might have been expected that increased enzyme activity would have been apparent. Activity of CuZnSOD can be reduced by glycation (57), which could lead to an increase in superoxide radicals. This may be the initial signal for the upregulation of mRNA expression to maintain steady-state activities. However, if nonenzymatic glycation affects CuZnSOD activity in VSMCs, why is it not affected in pericytes? Perhaps a more important inactivator may be free radical–induced enzymatic damage. In connection with this, Winyard et al. (58) have reported a decrease in the ferroxidase activity of ceruloplasmin incubated in the presence of free radicals; although this phenomenon has not been demonstrated yet for SOD, it could explain the findings in this work. The failure to demonstrate an increase in MnSOD enzymatic activity despite the increase in mRNA expression was somewhat unexpected. Because MnSOD resides within the mitochondria, glycation would seem to be an unlikely event; however, inactivation by increased superoxide radicals is probable.

The increase in MnSOD mRNA expression, in particular, is in keeping with its well-recognized induction in response to oxidative stress (27). Increased MnSOD mRNA expression has also been noted in endothelial cells cultured in high glucose concentrations (31), where glucose-induced oxidative stress is the most probable mechanism of induction. Increases in CuZnSOD mRNA levels have also been reported in endothelial cells cultured under high glucose conditions (31) and in kidneys from diabetic rats (59). When SOD activities are interpreted, it should be noted that the conditions of the standard assay give a 10-fold boost to the measured CuZnSOD activity with respect to that of MnSOD; in addition, the activities are normalized against total cell protein, which means that within the mitochondrial compartment, the actual superoxide scavenging activity/capacity of MnSOD is much higher than that of CuZnSOD in the cytoplasm. The failure to demonstrate an increase in mRNA levels of both catalase and GPX is in contrast to the increased levels demonstrated in endothelial cells (31). However, an increase in catalase mRNA expression might not be expected because the rate constant for the catalase enzyme is very high (~107 $[mmol/l]^{-1} \cdot s^{-1}$), implying that the enzyme is not easily saturated in vivo. In addition, catalase activity is confined to the peroxisomes, which are not specifically challenged by high
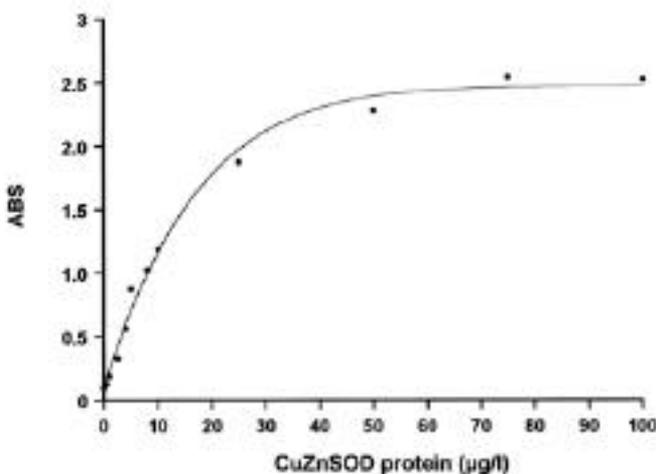
FIG. 5. Representative standard curve for ELISA measuring CuZnSOD protein concentration. Absorbance (ABS, 490 nm) versus CuZnSOD protein concentration (0–100 µg/l).
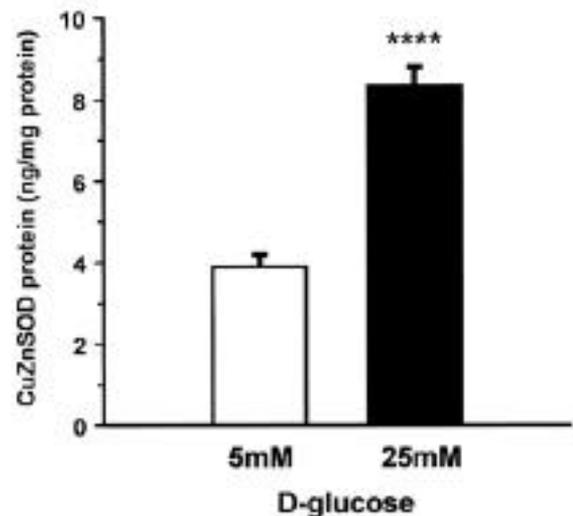

FIG. 6. CuZnSOD protein concentration (ng/mg protein) measured by ELISA in VSMCs cultured in 5 and 25 mmol/l D-glucose for 10 days. n = 15 independent experiments, each measured in duplicate. ****$P < 0.00001$.

rates of glucose metabolism. These results demonstrate, for the first time, the ability of the VSMC to respond to glucose-induced oxidative stress by increasing the mRNA levels of the SOD enzymes (both CuZnSOD and MnSOD).

There is an alternative explanation for the above findings: as previously discussed in detail, the depletion of GSH in both VSMCs and pericytes may be indicative of its consumption or usage under conditions of oxidative stress, and the failure to detect an increase in MDA in pericytes does not necessarily exclude the existence of free radical–induced damage to other cell components. Therefore, if GSH depletion alone can be taken as indicative of oxidative stress in both VSMCs and pericytes, it is interesting that there was a major difference in VSMCs and pericytes in their response to its existence. In contrast to VSMCs, pericytes were protected from lipid peroxidation and did not upregulate their gene expression of antioxidant enzymes.

In conclusion, this work has demonstrated that glucose causes significant changes in the antioxidant defenses of both VSMCs and pericytes. In both cell types, there is a major reduction of GSH levels. However, only in VSMCs—not in pericytes—are there increases in MDA, mRNA expression of CuZnSOD and MnSOD, and CuZnSOD protein concentration. The failure to detect an increase in CuZnSOD and MnSOD enzymatic activities in VSMCs may be related to inactivation by reactive oxygen species or nonenzymatic glycation. Under the experimental conditions used by us, the antioxidant profile of the pericyte, which had higher GSH concentrations in the cytosol and MnSOD activities in the mitochondria, appeared better able to deal with the increased free radical environment associated with high glucose concentrations. Pericytes did not show evidence of oxidant-induced damage in the form of lipid peroxidation, although both cell types demonstrated glucose-induced GSH depletion. The results suggest significant differences in the potential role of glucose-induced oxidative stress in the pathophysiology of vascular contractile cell dysfunction in diabetic macro- and microvasculopathy.

ACKNOWLEDGMENTS

REFERENCES

1. Stamler J, Vaccaro O, Neaton JD, Wentworth D: The Multiple Risk Factor Intervention Trial Research Group: diabetes, other risk factors and 12 years cardiovascular mortality for men screened in the Multiple Risk Factor Intervention Trial. *Diabetes Care* 16:434–444, 1993
2. Colwell JA: Vascular thrombosis in type 2 diabetes mellitus. *Diabetes* 42:8–11, 1993
3. Klein RR: The epidemiology of diabetic retinopathy. In *Textbook of Diabetes.* Vol. 2. Pickup J, Williams G, Eds. Oxford, U.K., Blackwell, 1991, p. 557–563
4. Anderson AR, Christiansen JS, Anderson JK, Kreiner S, Deckert T: Diabetic nephropathy in type 1 (insulin-dependent) diabetes: an epidemiological study. *Diabetologia* 25:496–501, 1983
5. The Diabetes Control and Complications Trial Research Group: The effect of intensive treatment of diabetes on the development and progression of long-term complications of insulin-dependent diabetes mellitus. *N Engl J Med* 329:977–986, 1993
6. Kuusisto J, Mykkanen L, Pyorala K, Laakso M: NIDDM and its metabolic control predict coronary heart disease in elderly subjects. *Diabetes* 43:960–967, 1994
7. McVeigh GE, Brennan GM, Johnston GD, McDermott BJ, McGrath LT, Henry WR, Andrews JW, Hayes JR: Impaired endothelium-dependent and independent vasodilation in patients with type 2 (non-insulin-dependent) diabetes mellitus. *Diabetologia* 35:771–776, 1992
8. Graier WF, Grubenthal I, Dittrich P, Wascher TC, Kostner GM: Intracellular mechanism of high D-glucose-induced modulation of vascular cell proliferation. *Eur J Pharmacol* 294:221–229, 1995
9. Pricci F, Pugliese G, Mene P, Romeo G, Romano G, Galli G, Casini A, Rotella CM, Dimario U, Pugliese F: Regulatory role of eicosanoids in extracellular matrix overproduction induced by long-term exposure to high glucose in cultured rat mesangial cells. *Diabetologia* 39:1055–1062, 1996
10. Li W, Shen S, Khatami M, Rockey JH: Stimulation of retinal capillary pericyte protein and collagen synthesis in culture by high glucose concentration. *Diabetes* 33:785–789, 1984
11. Ross R: The pathogenesis of atherosclerosis: an update. *N Engl J Med* 314:488–500, 1986
12. Oikawa S, Hayasaka K, Hashizume E, Kotake H, Midorikawa H, Sekikawa A, Kikuchi A, Toyota T: Human arterial smooth muscle cell proliferation in diabetes. *Diabetes* 45 (Suppl. 3):S114–S116, 1996
13. Cogan DG, Toussant D, Kuwabara T: Retinal vascular patterns. IV. Diabetic retinopathy. *Arch Ophthalmol* 66:366–378, 1961
14. Baynes JW: Role of oxidative stress in development of complications in diabetes. *Diabetes* 40:405–412, 1991
15. Hunt JV, Dean RT, Wolff SP: Hydroxyl radical production and autoxidative glycosylation: glucose autoxidation as the cause of protein damage in the experimental glycation model of diabetes mellitus and aging. *Biochem J* 256:205–212, 1988
16. Wolff SP, Dean RT: Glucose autoxidation and protein modification: the potential role of "autoxidative glycosylation" in diabetes. *Biochem J* 245:243–250, 1987
17. DeRubertis FR, Craven PA: Activation of protein kinase C in glomerular cells in diabetes: mechanisms and potential links to the pathogenesis of diabetic glomerulopathy. *Diabetes* 43:1–8, 1994
18. Williamson JR, Chang K, Frangos M, Hasan KS, Ido Y, Kawamura T, Nyengaard JR, van-den Enden M, Kilo C, Tilton RG: Hyperglycaemic pseudohypoxia and diabetic complications. *Diabetes* 42:801–813, 1993
19. Armstrong AM, Chestnutt JE, Gormley MJ, Young IS: The effect of dietary treatment on lipid peroxidation and antioxidant status in newly diagnosed non-insulin dependent diabetics. *Free Rad Biol Med* 21:719–726, 1996
20. Yoshida K, Hirokawa J, Tagami S, Kawakami Y, Urata Y, Kondo T: Weakened cellular scavenging activity against oxidative stress in diabetes mellitus: regulation of glutathione synthesis and efflux. *Diabetologia* 38:201–210, 1995
21. Velaquez E, Wincour PH, Kestsven P, Alberti KGMM, Laker MF: Relation of lipid peroxides to macrovascular disease in type 2 diabetes. *Diabet Med* 8:752–758, 1991
22. Griesmacher A, Kindhauser M, Andert SE, Schreiner W, Toma C, Knoebl P, Pietschmann P, Prager R, Schnack C, Schernthaner G, Mueller MM: Enhanced serum levels of thiobarbituric acid-reactive substances in diabetes mellitus. *Am J Med* 98:469–475, 1995
23. Zakowski JJ, Forstrom JW, Condell RA, Tappel AL: Attachment of selenocysteine in the catalytic site of glutathione peroxidase. *Biochem Biophys Res Comm* 84:248–253, 1978
24. Takahashi K, Cohen HJ: Selenium-dependent glutathione peroxidase protein and activity: immunological investigations on cellular and plasma enzymes. *Blood* 68:640–646, 1986
25. Clerch LB, Massaro D: Tolerance of rats to hyperoxia: lung antioxidant enzyme gene expression. *J Clin Invest* 91:499–508, 1993
26. Touati D: Regulation and protective role of the microbial superoxide dismutases. In *Current Communications in Cell and Molecular Biology. V. Molecular Biology and Free Radical Scavenging Systems.* Acandalios JG, Ed. Cold Spring Harbor, NY, Cold Spring Harbor, 1992, p. 231–261
27. Stralin P, Marklund SL: Effects of oxidative stress on expression of extracellular superoxide dismutase, CuZn-superoxide dismutase and Mn-superoxide dismutase in human dermal fibroblasts. *Biochem J* 298:347–352, 1994
28. Kong XJ, Lee SL, Lanzillo JJ, Fanburg BL: Cu,Zn superoxide dismutase in vascular cells: changes during cell cycling and exposure to hyperoxia. *Am J Physiol* 264:L365–L375, 1993
29. Keaney JF Jr, Xu A, Cunningham D, Jackson T, Frei B, Vita JA: Dietary probucol preserves endothelial function in cholesterol-fed rabbits by limiting vascular oxidative stress and superoxide generation. *J Clin Invest* 95:2520–2529, 1995
30. Curcio F, Ceriello A: Decreased cultured endothelial cell proliferation in high glucose medium is reversed by antioxidants: new insights on the pathophysiological mechanism of diabetic vascular complications. *In Vitro Cell Dev Biol* 28A:787–790, 1992
31. Ceriello A, dello Russo P, Amstad P, Cerutti P: High glucose induces antioxidant enzymes in human endothelial cells in culture: evidence linking hyper-

glycemia and oxidative stress. *Diabetes* 45:471–477, 1996

32. Gitlin JD, D'Amore PA: Culture of retinal capillary cells using selective growth media. *Microvasc Res* 26:74–80, 1983

33. Young IS, Trimble ER: Measurement of malondialdehyde in plasma by high performance liquid chromatography with fluorimetric detection. *Ann Clin Biochem* 28:504–508, 1991

34. McMaster D, Bell N, Anderson P, Love AHG: Automated measurement of two indicators of human selenium status, and applicability to population studies. *Clin Chem* 36:211–216, 1990

35. L'Abbe MR, Fischer PWF: An automated method for the determination of Cu,Zn-superoxide dismutase in plasma and erythrocytes using an ABA-200 discrete analyser. *Clin Biochem* 19:175–178, 1986

36. Sjostrom K, Crapo JD: Structural and biochemical adaptive changes in rat lungs after exposure to hypoxia. *Lab Invest* 48:68–78, 1983

37. Johansson LH, Borg LAH: A spectrophotometric method for determination of catalase activity in small tissue samples. *Anal Biochem* 174:331–336, 1988

38. Wheeler CR, Salzman JA, Elsayed NM, Omaye ST, Korte DW Jr: Automated assays for superoxide dismutase, catalase, glutathione peroxidase, and glutathione reductase activity. *Anal Biochem* 184:193–199, 1990

39. Griffith OW: Determination of glutathione and glutathione disulfide using glutathione reductase and 2-vinylpyridine. *Anal Biochem* 106:207–212, 1980

40. Chomczynski P, Sacchi N: Single-step method of RNA isolation by acid guanidinium thiocyanate-phenol-chloroform extraction. *Anal Biochem* 162:156–159, 1987

41. Akasaka M, Mizoguch J, Yoshimura S, Watanabe K: Nucleotide sequence of cDNA for rabbit glutathione peroxidase. *Nucleic Acids Res* 17:2136, 1989

42. Gunzler WA, Steffens GJ, Grossman A, Kim SMA, Otting F, Wendel A, Flohe L: The amino-acid sequence of bovine glutathione peroxidase. *Hoppe-Seyler's Z Physiol Chem* 365:195–212, 1984

43. Takahashi K, Akasaka M, Yamamoto Y, Kobayashi C, Mizoguchi J, Koyama J: Primary structure of human plasma glutathione peroxidase deduced from cDNA sequences. *J Biochem* 108:145–148, 1990

44. Esterbauer H, Dieber-Rotheneder M, Striegl G, Waeg G: Role of vitamin E in preventing the oxidation of low-density lipoprotein. *Amer J Clin Nutr* 53:314S–321S, 1991

45. Suzuki Y, Lyall V, Biber TUL, Ford GD: A modified technique for the measurement of sulphydryl groups oxidized by reactive oxygen intermediates. *Free Rad Biol Med* 9:479–484, 1990

46. Teare JP, Punchard NA, Powell JJ, Lund PJ, Mitchell WD, Thompson RPH: Automated spectrophotometric method for determining oxidised and reduced glutathione in liver. *Clin Chem* 39:686–689, 1993

47. Cameron NE, Cotter MA, Maxfield EK: Antioxidant treatment prevents the development of peripheral nerve dysfunction in streptozotocin-diabetic rats. *Diabetologia* 36:299–304, 1993

48. Kondo T, Kawakami Y, Taniguchi N, Beutler E: Glutathione disulfide-stimulated Mg^{2+}-ATPase of human erythrocyte membranes. *Proc Natl Acad Sci USA* 84:7373–7377, 1987

49. Meister A: Metabolism and function of glutathione. In *Glutathione: Chemical, Biochemical and Medical Aspects*. Dolphin D, Poulson R, Avramovic O, Eds. New York, John Wiley, 1989, p. 367–474

50. Srivastava SK, Beutler E: The transport of oxidised glutathione from human erythrocytes. *J Biol Chem* 244:9–16, 1969

51. Ishikawa T, Sies H: Cardiac transport of glutathione disulfide and S-conjugate: studies with isolated perfused rat heart during hydroperoxide metabolism. *J Biol Chem* 259:3838–3843, 1984

52. Chari SW, Nath N, Rathi AB: Glutathione and its redox system in diabetic polymorphonuclear leukocytes. *Am J Med Sci* 287:14–15, 1984

53. Thomas G, Skrinska V, Lucas FV, Schumacher OP: Platelet glutathione and thromboxane synthesis in diabetes. *Diabetes* 34:951–954, 1985

54. Murakami K, Kondo T, Ohtsuka Y, Fujiwara Y, Shimada M, Kawakami Y: Impairment of glutathione metabolism in erythrocytes from patients with diabetes mellitus. *Metabolism* 38:753–758, 1989

55. Trocino RA, Akazawa S, Ishibashi M, Matsumoto K, Matsuo H, Yamamoto H, Goto S, Urata Y, Kondo T, Nagataki S: Significance of glutathione depletion and oxidative stress in early embryogenesis in glucose-induced rat embryo culture. *Diabetes* 44:992–998, 1995

56. Turrens JF, Boveris A: Generation of superoxide anion by the NADH dehydrogenase of bovine heart mitochondria. *Biochem J* 191:421–427, 1980

57. Arai K, Iizuka S, Tada Y, Oikawa K, Taniguchi N: Increase in the glucosylated form of erythrocyte CuZn superoxide dismutase in diabetes and close association of the nonenzymatic glucosylation with the enzyme activity. *Biochim Biophys Acta* 924:292–296, 1987

58. Winyard PG, Hider RC, Brailsford S, Drake AF, Lunec J, Blake DR: Effects of oxidative stress on some physicochemical properties of ceruloplasmin. *Biochem J* 258:435–445, 1989

59. Sechi LA, Ceriello A, Griffin CA, Catena C, Amstad P, Schambelan M, Bartoli E: Renal antioxidant enzyme mRNA levels are increased in rats with experimental diabetes mellitus. *Diabetologia* 40:23–29, 1997